REPORT DOCUMENTATION PAGE

Form Approved OMB NO. 0704-0188

The public reporting burden for this collection of information is estimated to average 1 hour per response, including the time for reviewing instructions, searching existing data sources, gathering and maintaining the data needed, and completing and reviewing the collection of information. Send comments regarding this burden estimate or any other aspect of this collection of information, including suggesstions for reducing this burden, to Washington Headquarters Services, Directorate for Information Operations and Reports, 1215 Jefferson Davis Highway, Suite 1204, Arlington VA, 22202-4302. Respondents should be aware that notwithstanding any other provision of law, no person shall be subject to any oenalty for failing to comply with a collection of information if it does not display a currently valid OMB control number.
PLEASE DO NOT RETURN YOUR FORM TO THE ABOVE ADDRESS.

1. REPORT DATE (DD-MM-YYYY)	2. REPORT TYPE	3. DATES COVERED (From - To)
	New Reprint	-

4. TITLE AND SUBTITLE

176. Effect of selective Co addition on magnetic properties of Nd2(FeCo)14B/?-Fe nanocomposite magnets

5a. CONTRACT NUMBER
W911NF-11-1-0507

5b. GRANT NUMBER

5c. PROGRAM ELEMENT NUMBER
611102

6. AUTHORS

C. Bing Rong, Dapeng Wang, Vuong Van Nguyen, Maria Daniil, Matthew A. Willard, Ying Zhang, M. J. Kramer, and J. Ping Liu

5d. PROJECT NUMBER

5e. TASK NUMBER

5f. WORK UNIT NUMBER

7. PERFORMING ORGANIZATION NAMES AND ADDRESSES

University of Texas at Arlington
Research Administration
701 S. Nedderman Dr., Box 19145
Arlington, TX 76019 -0145

8. PERFORMING ORGANIZATION REPORT NUMBER

9. SPONSORING/MONITORING AGENCY NAME(S) AND ADDRESS(ES)

U.S. Army Research Office
P.O. Box 12211
Research Triangle Park, NC 27709-2211

10. SPONSOR/MONITOR'S ACRONYM(S)
ARO

11. SPONSOR/MONITOR'S REPORT NUMBER(S)
60580-MS.7

12. DISTRIBUTION AVAILIBILITY STATEMENT

Approved for public release; distribution is unlimited.

13. SUPPLEMENTARY NOTES

The views, opinions and/or findings contained in this report are those of the author(s) and should not contrued as an official Department of the Army position, policy or decision, unless so designated by other documentation.

14. ABSTRACT

176. Effect of selective Co addition on magnetic properties of Nd2(FeCo)14B/?-Fe nanocomposite magnets, C. Bing Rong, Dapeng Wang, Vuong Van Nguyen, Maria Daniil, Matthew A. Willard, Ying Zhang, M. J. Kramer, and J. Ping Liu, J. Phys. D: Appl. Phys., 46 (2013) 045001 (5pp).

15. SUBJECT TERMS

Nanocomposite magnets

16. SECURITY CLASSIFICATION OF:			17. LIMITATION OF ABSTRACT	15. NUMBER OF PAGES	19a. NAME OF RESPONSIBLE PERSON
a. REPORT	b. ABSTRACT	c. THIS PAGE			J. Ping Liu
UU	UU	UU	UU		19b. TELEPHONE NUMBER: 817-272-2815

Report Title

176. Effect of selective Co addition on magnetic properties of Nd2(FeCo)14B/?-Fe nanocomposite magnets

ABSTRACT

176. Effect of selective Co addition on magnetic properties of Nd2(FeCo)14B/?-Fe nanocomposite magnets, C. Bing Rong, Dapeng Wang, Vuong Van Nguyen, Maria Daniil, Matthew A. Willard, Ying Zhang, M. J. Kramer, and J. Ping Liu, J. Phys. D: Appl. Phys., 46 (2013) 045001 (5pp).

REPORT DOCUMENTATION PAGE (SF298)
(Continuation Sheet)

Continuation for Block 13

ARO Report Number 60580.7-MS
176. Effect of selective Co addition on magne ...

Block 13: Supplementary Note
© 2012 . Published in , Vol. Ed. 0 (2012), (Ed.). DoD Components reserve a royalty-free, nonexclusive and irrevocable right to reproduce, publish, or otherwise use the work for Federal purposes, and to authroize others to do so (DODGARS §32.36). The views, opinions and/or findings contained in this report are those of the author(s) and should not be construed as an official Department of the Army position, policy or decision, unless so designated by other documentation.

Approved for public release; distribution is unlimited.

IOP PUBLISHING JOURNAL OF PHYSICS D: APPLIED PHYSICS

J. Phys. D: Appl. Phys. **46** (2013) 045001 (5pp) doi:10.1088/0022-3727/46/4/045001

Effect of selective Co addition on magnetic properties of $Nd_2(FeCo)_{14}B/\alpha$-Fe nanocomposite magnets

C Bing Rong[1], Dapeng Wang[1], Vuong Van Nguyen[1], Maria Daniil[2], Matthew A Willard[3], Ying Zhang[4], M J Kramer[4] and J Ping Liu[1]

[1] Department of Physics, University of Texas at Arlington, Arlington, TX 76019, USA
[2] Department of Physics, George Washington University, Washington, DC 20052, USA
[3] Naval Research Laboratory, Code 6355, 4555 Washington, DC 20375, USA
[4] Ames Laboratory of USDOE, Iowa State University, Ames, IA 50011, USA

E-mail: pliu@uta.edu

Received 17 July 2012, in final form 11 October 2012
Published 13 December 2012
Online at stacks.iop.org/JPhysD/46/045001

Abstract

$Nd_2Fe_{14}B/\alpha$-Fe-based hard/soft nanocomposite magnets with Co addition have been prepared by ball-milling and warm compaction. It was found that Co addition into the magnetically hard phase improves magnetic properties significantly, especially the remanence ratio and coercivity. The effect on the magnetic properties of the selective Co addition may be attributed to enhanced interdiffusion across the hard/soft interface that improves the interface conditions for effective interphase exchange coupling. By optimizing the Co content in the $Nd_{15}Fe_{79-x}Co_xB_6$ hard phase, an energy product value about 21 MG Oe can be obtained in the isotropic $Nd_2(FeCo)_{14}B/\alpha$-(FeCo) nanocomposite magnets compared with 15 MG Oe of $Nd_2Fe_{14}B/\alpha$-Fe nanocomposite magnets prepared under the same conditions with the same grain size and microstructure, owing to the strengthened intergranular exchange interactions.

(Some figures may appear in colour only in the online journal)

Increased demand for rare-earth permanent magnets coupled with shortages in rare-earth supply, especially the Nd–Fe–B based magnets for traction motor and wind turbine applications, necessitates reduction in the rare-earth content in these materials [1, 2]. Exchange-coupled hard/soft nanocomposite permanent magnets are a suitable approach to achieve this goal since the addition of a magnetically soft phase reduces the rare-earth content while enhancing the energy density by combining the large magnetocrystalline anisotropy of the hard phase and large magnetic flux density of the soft phase [3–6]. The exchange-coupled nanocomposite magnets have the potential to double the energy products of the Nd–Fe–B single-phase magnets [4]. Our recent experimental work has demonstrated that energy product enhancement greater than 100% is achieved in Sm–Co/Fe nanocomposites with up to 30% of the Fe-based soft phase [7–9]. A prerequisite for the effective interphase exchange coupling is a homogeneous distribution of the soft phase with grain size smaller than a critical length (~10 nm) [3–6, 10–12]. In addition, previous simulation and experimental investigations have shown that the grain boundaries with graded composition profiles promote exchange coupling between the hard and soft phases [13–19].

The effect of Co addition on magnetic properties of the $Nd_2Fe_{14}B$ single phase has been extensively studied since the initial discovery of the Nd–Fe–B magnets [20–27]. It was found that Co substitution of Fe in the tetragonal phase greatly increases the Curie temperature while having minimal deleterious effects on the magnetization, magnetocrystalline anisotropy and coercivity. Chang *et al* [28] have investigated the effect of Co substitutions for Fe on magnetic properties of melt-spun $Nd_2Fe_{14}B/\alpha$-Fe nanocomposite magnets and found that increasing Co content promoted grain coarsening with simultaneously enhanced exchange coupling. However, the underlying mechanism of these effects remains unclear.

Unlike melt-spin processing, where partitioning on the various magnetic and possibly non-magnetic phases is a complex relationship between undercooling controlled by wheel speed and composition, mechanical milling

 © 2013 IOP Publishing Ltd Printed in the UK & the USA

allows for controlled addition of soft phases to the hard phase. Subsequent solid-state, high pressure compaction (i.e. warm compaction) of the ball milled constituents into a nanocomposite magnet has been found to better control the interfacial properties in the Sm–Co/Fe system [7, 8]. In this paper, we report structural and magnetic properties for the $Nd_2(Fe,Co)_{14}B/\alpha$-Fe nanocomposite system using a similar processing approach.

Ingots of $Nd_{15}Fe_{79-x}Co_xB_6$ (x = 0–50) were prepared from high purity elemental constituents by arc melting under UHP argon. The $Nd_{15}Fe_{79-x}Co_xB_6$ ingots were further processed by grinding into powder samples with a size of ~45 μm. Commercial α-Fe powder samples with a size of ~10 μm were mixed together with the hard-phase powder and milled in a SPEX 8000M high-energy ball mill to form the nanocomposites. The weight ratio of soft phase to hard phase (denoted as y) was varied from 0% to 40%. The milling conditions included: 440 °C hardened steel balls, with a weight ratio of sample : balls ~1 : 20–30, and milling times from 0.5 to 10 h. The as-milled powders were then annealed at temperatures from 525 to 600 °C under vacuum for 0.5 h. The optimal magnetic properties were found for a milling time of 4 h and annealing temperature of 550 °C. These are the default experimental conditions in this work if not otherwise specified. The annealed powders were then compacted using a warm compaction technique [29] at 500 °C under a quasi-isostatic pressure of ~2.5 GPa. The final bulk magnets having dimensions Ø6 mm × 1.5 mm were characterized for morphology and the crystalline structure using scanning electron microscopy (SEM), transmission electron microscopy (TEM), energy-filtered TEM (EFTEM) and x-ray diffraction (XRD) using Cu K_α radiation. Magnetic properties were measured with a superconducting quantum interference device (SQUID) magnetometer with a maximum applied field of 70 kOe. To calculate the true energy product $(BH)_{max}$ of the bulk sample, we determined the demagnetization factor experimentally as described in [9]. Figure 1 shows the XRD patterns of the as-milled and annealed matrix-phase $Nd_{15}Fe_{79}B_6$ (mostly the 2 : 14 : 1 phase) and the two-phase nanocomposite prepared from the mixture of $Nd_{15}Fe_{79}B_6$ + 20 wt% α-Fe powders (y = 20). The patterns of both samples show very broadened peaks around 45° and 65° two theta, which is from a typical body-centred-cubic (bcc) structure, indicating that the as-milled NdFeB alloy consists of amorphous and bcc structured α-Fe phases. The XRD patterns of the annealed powders show that the 2 : 14 : 1 tetragonal structure was developed during the post-annealing at 550 °C for 0.5 h. In addition, the α-Fe peaks were also observed in the two-phase system, indicating that a nanocomposite NdFeB/α-Fe was obtained after appropriate ball milling and post-annealing. It should be noted that the content of the soft phase will be somehow reduced after the annealing due to the equilibrium conditions. The $Nd_{15}Fe_{79-x}Co_xB_6/\alpha$-Fe powders with varying Co content have very similar XRD patterns, as shown in figure 1.

Figure 2 shows the demagnetization curves of the nanocomposite magnets prepared from the mixture of $Nd_{15}Fe_{79-x}Co_x$ B_6 + 20 wt% α-Fe compacted from the annealed powders. It should be noted that maximum measuring magnetic field of 70 kOe was sufficient to saturate the samples, although the figure only shows a limited range of magnetic field. The coercivity of the nanocomposite magnet without Co substitution (x = 0) is only about 5.3 kOe. One can see clearly that the coercivity increases to 6.2 and 8.3 kOe just by increasing the Co content x in the $Nd_{15}Fe_{79-x}Co_xB_6$ raw materials in steps from 0 to 10 and 15, respectively. The remanence also increases from 97 to 108 emu g^{-1} by increasing

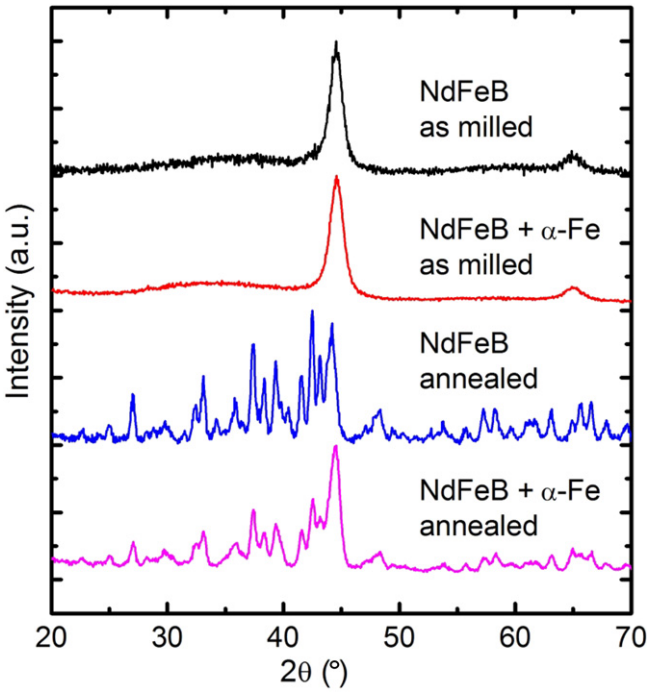

Figure 1. XRD patterns of as-milled $Nd_{15}Fe_{79}B_6$ and $Nd_{15}Fe_{79}B_6$ + 20 wt% α-Fe powders (the upper two) and the powders annealed at 550 °C for 0.5 h (the lower two). The upper patterns show only α-Fe peaks and the lower patterns show the $Nd_2Fe_{14}B$ peaks and the lowest pattern show both phases.

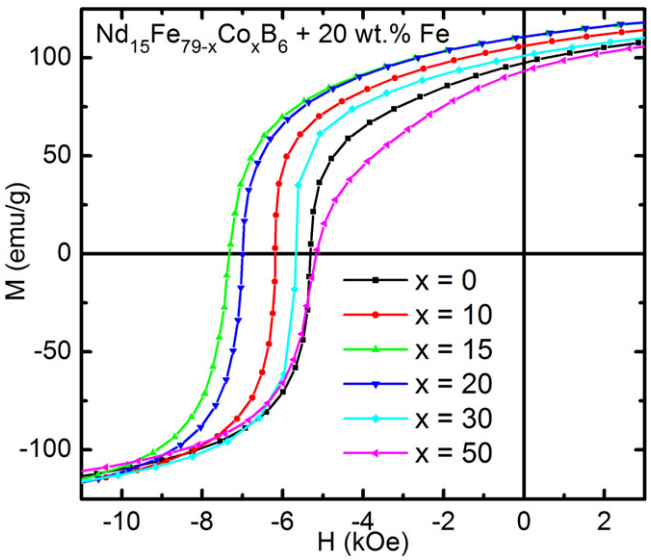

Figure 2. Demagnetization curves of the $Nd_{15}Fe_{79-x}Co_xB_6$ + 20 wt% α-Fe nanocomposite magnets with variation of Co content in the ingot hard-phase alloy.

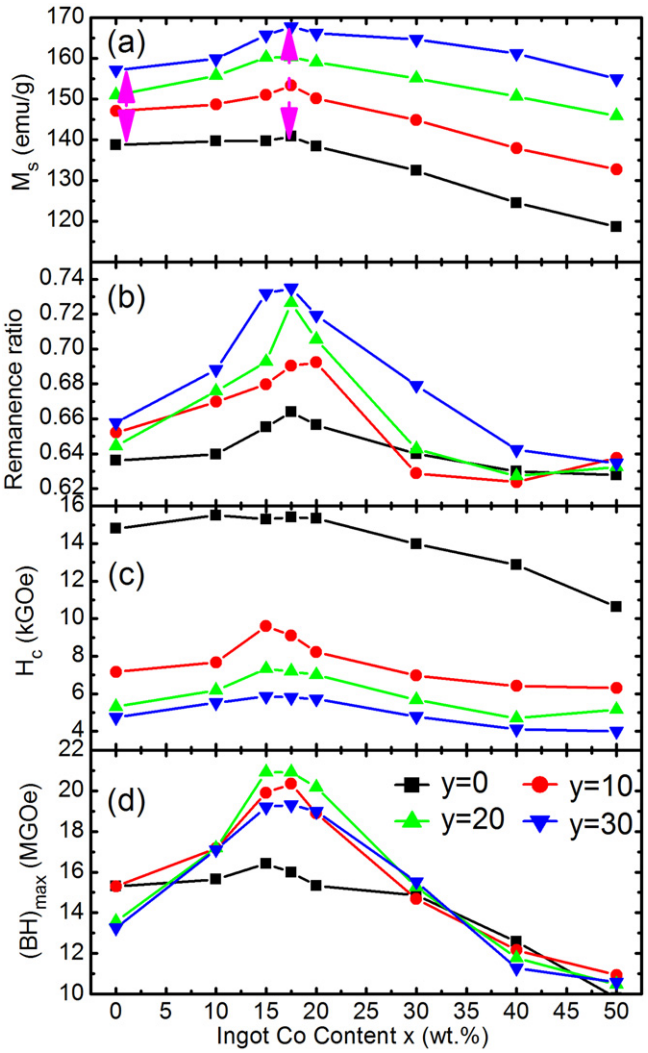

Figure 3. Dependence of (*a*) saturation magnetization (M_s), (*b*) remanence ratio, (*c*) coercivity (H_c) and (*d*) energy product ($(BH)_{max}$) on the Co content in $Nd_{15}Fe_{79-x}Co_xB_6$ + ywt% α-Fe. The soft-phase α-Fe content y changes from 0% to 30 wt%.

x from 0 to 15. In addition, the squareness of demagnetization curves was significantly improved with increasing x, implying that Co addition, in this range, leads to enhanced exchange coupling between the hard and soft phases. The figure also shows that further increase in Co led to a decreased coercivity, magnetization and loop squareness, which is understandable in view of the lower magnetization and anisotropy of the $Nd_2Co_{14}B$ phase [22–24].

Figure 3 summarizes the dependence of saturation magnetization (M_s), remanence ratio (M_r/M_s), coercivity (H_c) and energy product ($(BH)_{max}$) on x in the $Nd_{15}Fe_{79-x}Co_xB_6/\alpha$-Fe nanocomposite magnets with different soft-phase fractions. It is interesting to see that alloying with Co significantly increases M_s, M_r/M_s, H_c and thus $(BH)_{max}$ of the nanocomposite magnets in the range of $0 < x < 17.5$ at%. As shown in figure 3(*a*), the difference of M_s between $Nd_{15}Fe_{79}B_6$ and $Nd_{15}Fe_{79}B_6$ + 30 wt%α-Fe magnets (initial composition), $\Delta M_{x=0}$, is 18.4 emu g^{-1}, while that of the system with Co addition of $x = 17.5$, $\Delta M_{x=17.5}$ is about 26.9 emu g^{-1}. The remarkable enhancement in M_s (about 8.5 emu g^{-1}) upon the Co addition may be attributed to the formation of high magnetization FeCo phase due to the diffusion of Co from the $Nd_2(FeCo)_{14}B$ phase into the α-Fe soft phase, as we observed in the SmCo/α-Fe systems processed in the same techniques [7–9]. More interestingly, figure 3(*b*) shows that Co addition increases the remanence ratio significantly. For example, the remanence ratio of the nanocomposite magnets with 30 wt% α-Fe increases from 0.66 to 0.73 upon Co addition of $x = 17.5$, indicating enhanced exchange coupling. In addition, figure 3(*c*) shows that Co addition in the hard phase also enhances the coercivity of the final nanocomposite magnets. As one can see that H_c was only increased by 0.6 kOe for the matrix-phase magnet ($y = 0$), from 14.8 to 15.4 kOe when 17.5% Co was added. Surprisingly, H_c of the nanocomposite magnets with $y = 10$ and 20 increased by 2.4 kOe and 2.0 kOe respectively with addition of Co of the same percentage. As a result of the remarkably enhanced remanence and coercivity, energy product of the composite magnets is substantially increased upon the Co substitution. As shown in figure 3(*d*), $(BH)_{max}$ of nanocomposite magnets prepared with 20 wt% α-Fe reaches the peak value of 20.9 MG Oe (from 13.6 MG Oe for $x = 0$) as Co is substituted for Fe in the Nd(Fe,Co)B ingots. For comparison, the $(BH)_{max}$ of the matrix-phase magnets only increases from 15.8 to 16.2 MG Oe with the same Co change. It can also be seen from figure 3 that all of the magnetic properties deteriorate for ingot Co content (x) exceeding 20%, for the reason mentioned above that Co substitution for Fe in the $Nd_2(Fe,Co)_{14}B$ phase deteriorates both the saturation magnetization and anisotropy when substitutions exceed about 14 at% [22–24].

It should be noted that our results for Co addition on the matrix-phase magnets (mostly the 2 : 14 : 1 phase) are in accordance with previously reported results (figure 3) [20–27], initially little change in B_r and M_s are observed followed by abruptly decreasing values at Co contents greater than ~20 at%. However, the effect of Co addition (in the hard phase) on the composite systems is very significant. The observed improvement of the magnetic properties in the nanocomposite system in comparison with the matrix-phase magnets implies the importance of interdiffusion of the transition metal between the hard and the soft phases. It is likely that this remarkable effect in nanocomposite systems is based more on the microstructure of the magnets, instead of just on the intrinsic properties of the hard-phase component in the composite systems. However, it is also possible that the reduced anisotropy of the matrix phase upon Co doping has led to an increased exchange length in the nanocomposite which facilities the interphase exchange coupling, as reported in [26].

In order to verify this idea, we also tested Co addition in both phases and/or just in the soft phase. Results showed that the effect in the latter cases is not as significant as for the effect shown in figures 2 and 3. A reasonable inference is that the *selective* addition into the hard phase results in enhanced interdiffusion of Co atoms from the $Nd_2(FeCo)_{14}B$ phase into α-Fe phase. This kind of diffusion should modify the interphase interface conditions in the nanocomposite that favour interphase exchange coupling, as we reported previously [13–16]. To confirm this

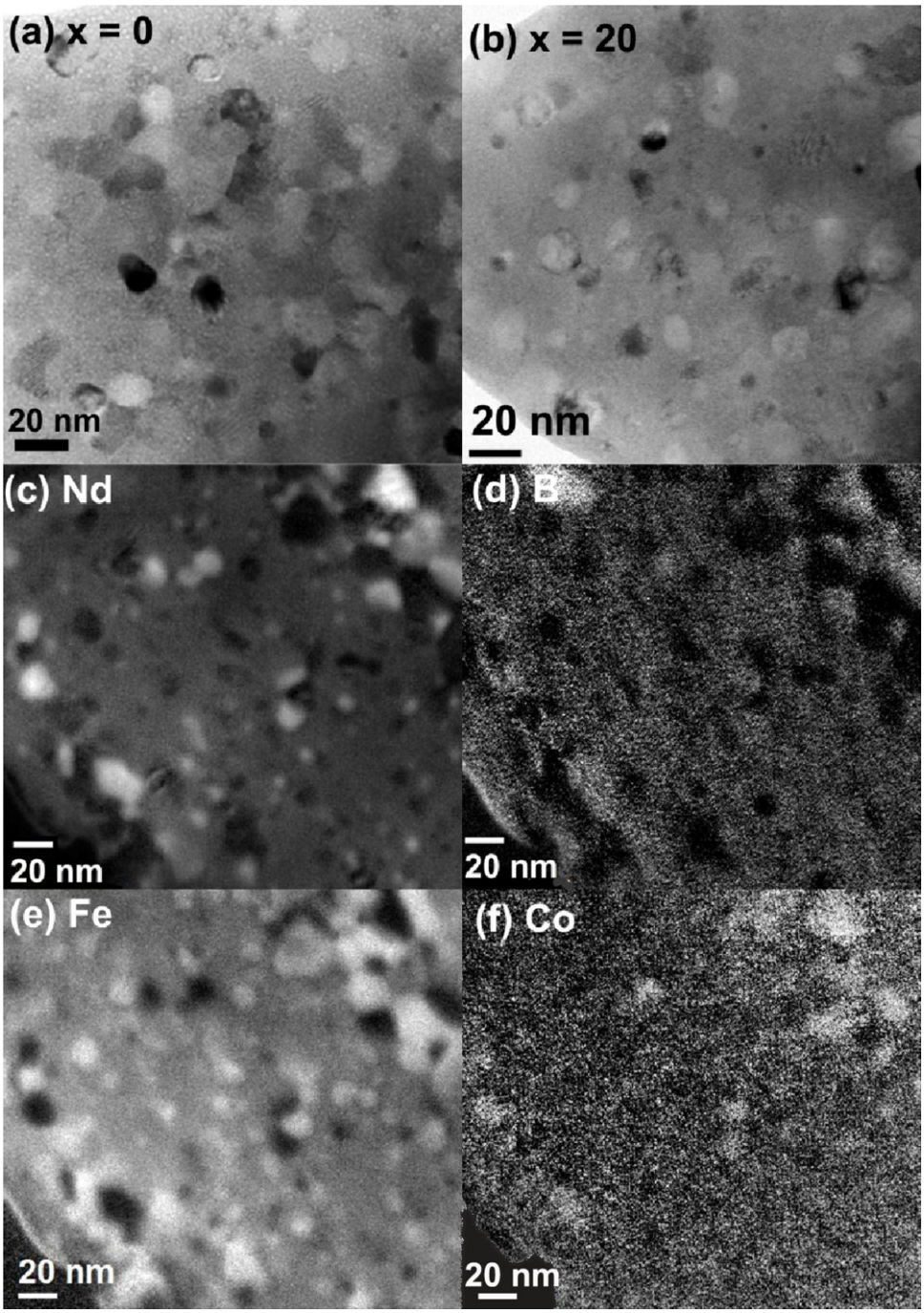

Figure 4. Bright field images of $Nd_{15}Fe_{79-x}Co_xB_6$ + 20 wt% α-Fe nanocomposite magnets with (*a*) $x = 0$ and (*b*) $x = 20$ and the element mapping of (*c*) Nd, (*d*) B, (*e*) Fe and (*f*) Co of the nanocomposite magnets with $x = 20$.

assumption, microstructure observations by TEM were performed. Figure 4 shows the TEM and energy-filtered TEM (element mapping) of the nanocomposite magnets with and without Co additions. The findings can be summarized as follows:

(1) the addition of Co does not affect grain size of the nanocomposite magnets. The grain size of both Co-free and Co-containing alloys is very similar and under 20 nm (see figures 4(*a*) and (*b*)).

(2) the soft-phase distribution of both systems is also similarly homogeneous according to the elemental mapping analysis (see Fe map in figure 4(*e*); the Fe map of Co-free nanocomposite magnet is not shown here). In addition, the grain size of most α-Fe grains is around 10 nm (see figure 4(*e*)), which ensures an effective exchange coupling according to the models [3–6, 10–12].

(3) The Co distribution is homogeneous in most areas. This homogeneity may be facilitated by the extensive Co/Fe diffusion during the 0.5 h warm compaction process. The homogeneity of the Co distribution may be due to that fact that Co has diffused from the $Nd_2(FeCo)_{14}B$ phase into α-Fe phase to form an α-(FeCo) phase since only pure iron was added into the system prior to ball milling.

This diffusion process may lead to formation of a smooth transition region across the interphase interfaces between the $Nd_2(FeCo)_{14}B$ and the α-(FeCo) phases. Therefore, it is understandable that the addition of Co to the hard phase in the alloy improves the saturation magnetization, the remanence ratio, the coercivity and thus the energy product, because of the enhanced interphase exchange coupling.

(4) Some Nd-rich areas are observed in figure 4(*c*). However, these areas are not really Nd-rich phase after a careful comparison between figures 4(*c*) and 4(*f*). As one can see that the 'Nd-rich' areas are always associated with high Co and high B content but low Fe content, indicating that these areas might be the 1 : 4 : 4 boride grains. These areas have relatively large grain size compared with other Nd(FeCo)B grains so that less Co has been diffused out. These larger grains tend to have brighter intensity observed in the Co maps, indicating higher Co enrichment. For this reason, we believe that the magnetic properties of $Nd_2(FeCo)_{14}B/\alpha$-Fe nancomposite magnets could be further improved if a more homogeneous nanostructure could be obtained.

In summary, $Nd_2(FeCo)_{14}B/\alpha$-Fe nanocomposite magnets have been prepared by a novel processing route. The effect of Co addition on the structural and magnetic properties of nanocomposite magnets have been investigated. The maximum energy product about 21 MG Oe was obtained in $Nd_{15}Fe_{79-x}Co_xB_6$ + ywt% α-Fe nanocomposite magnets (with $x = 17.5$ and $y = 20$), in comparison with ~13 MG Oe in the Co-free nanocomposite counterparts with the similar grain sizes and soft-phase distribution. More interestingly, addition of Co into each phase or just the soft phase alone does not result in the same performance enhancement. According to the magnetic property and TEM analyses, Co addition into the $Nd_2Fe_{14}B$ hard phase may have resulted in interdiffusion of the transition metals which leads to enhanced magnetization of the soft phase as well as strengthened exchange coupling between the two phases. This investigation reveals a fact that the same doping elements give rise to substantially different effects on single-phase materials and composite materials, which is significant for the future nanocomposite magnet fabrication.

Acknowledgments

This work has been supported in part by the DARPA/ARO under grant W911NF-08-1-0249 and ARO under grant W911NF-11-1-0507. The microscopy was performed at the Ames Laboratory, which is supported in part by the US Department of Energy, Office of Basic Energy Science, under contract DE-AC02-07CH11358.

References

[1] 2010 Critical Materials Strategy, US Department of Energy, http://www.energy.gov/news/documents/criticalmaterialsstrategy.pdf
[2] Gutfleisch O, Willard M A, Bruck E, Chen C H, Sankar S G and Liu J P 2011 *Adv. Mater.* **23** 821
[3] Kneller E F and Hawig R 1991 *IEEE Trans. Magn.* **27** 3588
[4] Skomski R and Coey J M D 1993 *Phys. Rev.* B **48** 15812
[5] Fischer R, Schrefl T, Kronmuller H and Fidler J 1995 *J. Magn. Magn. Mater.* **150** 329
[6] Rong C B, Zhang H, Chen R, He S and Shen B 2006 *J. Magn. Magn. Mater.* **302** 126
[7] Rong C B, Zhang Y, Poudyal N, Xiong X, Kramer M J and Liu J P 2010 *Appl. Phys. Lett.* **96** 102513
[8] Zhang Y, Kramer M J, Rong C B and Liu J P 2010 *Appl. Phys. Lett.* **97** 032506
[9] Rong C B, Zhang Y, Poudyal N, Szlufarska I, Hebert R J, Kramer M J and Liu J P 2011 *J. Mater. Sci.* **46** 6065
[10] Krommuler H, Fisher R, Bachmann M and Leinewber T 1999 *J. Magn. Magn. Mater.* **203** 12
[11] Shan Z S, Liu J P, Chakka V M, Zeng H and Jiang J S 2002 *IEEE Trans. Magn.* **38** 2907
[12] Guo Z J, Jiang J S, Pearson J E, Bader S D and Liu J P 2002 *Appl. Phys. Lett.* **81** 2029
[13] Jiang J S *et al* 2004 *Appl. Phys. Lett.* **85** 5293
[14] Choi Y *et al* 2007 *Phys. Rev.* B **75** 104432
[15] Choi Y, Jiang J S, Pearson J E, Bader S D, Kavich J, Freeland J W and Liu J P 2007 *Appl. Phys. Lett.* **91** 072509
[16] Wu D, Zhang Q, Liu J P and Sabirianov R F 2008 *J. Nanosci. Nanotechnol.* **8** 3036
[17] Zhang X Y, Guan Y, Zhang J W, Sprengel W, Reichle K J, Blaurock K, Reimann R and Schaefer H E 2002 *Phys. Rev.* B **66** 212103
[18] Zhang X Y, Guan Y and Zhang J W 2002 *Appl. Phys. Lett.* **80** 1966
[19] Li W, Li X, Li L, Zhang J and Zhang X 2006 *J. Appl. Phys.* **99** 126103
[20] Sagawa M, Fujimura S, Yamamoto H, Matsuura Y and Hiraga K 1984 *IEEE. Trans. Magn.* **MAG-20** 1584
[21] Yang Y, Ho W, Chen H, Wang J and Lan J 1985 *J. Appl. Phys.* **57** 4118
[22] Huang M Q, Boltich E B and Wallace W E 1986 *J. Magn. Magn. Mater.* **60** 270
[23] Fuerst C D and Herbst J F 1989 *J. Appl. Phys.* **66** 1782
[24] Wecker J and Schultz L 1989 *J. Magn. Magn. Mater.* **80** 97
[25] Liu Z W and Davies H a 2006 *J. Phys. D: Appl. Phys.* **39** 2647
[26] Neu V and Schultz L 2001 *J. Appl. Phys.* **90** 1540
[27] Bollero A, Gutfleisch, Muller K H and Schultz L 2002 *J. Appl. Phys.* **91** 8159
[28] Chang W C, Wu S H, Ma B M, Bounds C O and Yao S Y 1998 *J. Appl. Phys.* **83** 2147
[29] Rong C B, Zhang Y, Poudyal N, Wang D, Kramer M J and Liu J P 2011 *J. Appl. Phys.* **109** 07A735